SCIENCE CHINA
Chemistry

• ARTICLES • February 2011 Vol.54 No.2: 397–404
• SPECIAL ISSUE • In Honor of the 80th Birthdays of Professors SHEN JiaCong, SHEN ZhiQuan and ZHUO RenXi doi: 10.1007/s11426-010-4191-9

Graphene nanosheets decorated with Pd, Pt, Au, and Ag nanoparticles: Synthesis, characterization, and catalysis applications

HE HongKun & GAO Chao*

MOE Key Laboratory of Macromolecular Synthesis and Functionalization; Department of Polymer Science and Engineering, Zhejiang University, Hangzhou 310027, China

Received July 14, 2010; accepted August 3, 2010

We report that noble metal nanopartcles (Pd, Pt, Au, and Ag) decorated-graphene nanosheets can be synthesized with the template of graphene oxide by a one-pot solution-based method. The resulting hybrid materials are characterized by transmission electronic microscopy, energy dispersive X-ray spectroscopy, scanning electronic microscopy, atomic force microscopy, X-ray diffraction, and Raman spectroscopy, which demonstrate that the metal nanoparticles have been uniformly deposited on the surfaces of graphene nanosheets. Our results in turn verify that the carboxylic groups of graphene oxide are statistically distributed on its whole sheet surface rather than just at its edges. The graphene-metal nanohybrids can be used as catalysts in the reduction of potassium hexacyanoferrate(III) with $NaBH_4$ in aqueous solution. Our results suggest that graphene is a superior substrate to support metals for applications in the heterogeneous catalysis.

graphene, graphene oxide, noble metal nanoparticles, hybrids, catalyst

1 Introduction

Graphene represents a new class of carbon material that is formed by sp^2 bonded carbon atoms arranged in a single-layer hexagonal lattice. The research about graphene is currently a hot topic in the scientific community due to its unique nanostructure and fascinating properties [1–8]. The two-dimensional (2-D) basal plane structure and high specific surface area (calculated value, 2630 m^2/g) make graphene an ideal substrate for supporting catalytic nanoparticles [9–11].

Noble metal nanoparticles (NPs) have been widely used as catalysts to promote various chemical reactions [12, 13]. Catalyst support is an important aspect that could greatly influence the catalysis effect [14]. In order to enhance the catalysis efficiency of noble metal NPs, many materials have been utilized as catalyst supports. Carbon material is a typical example of the extensively studied supports. For example, Pd/C (palladium metal supported on charcoal) is an efficient catalyst for hydrogenation, hydrogenolysis, carbon-carbon bond formation [15]. Carbon nanofibers (CNFs) have cylindric nanostructures and are suitable to be used as catalysts supports [16, 17]. The quasi one-dimensional (1-D) tubular carbon nanomaterials, carbon nanotubes (CNTs), have been widely studied as stabilizers and supporters for metal NPs due to their unique structural, electrical, and mechanical properties [18, 19]. In comparison with the 1-D CNTs, the 2-D graphene has larger specific surface area and could be obtained more easily and inexpensively. Therefore, since its discovery in 2004 [20], graphene has been used as support material for the deposition of metal NPs for potential utilizations in catalysts [21, 22], fuel cells [23–27], biosensors [28, 29], spectroscopic

*Corresponding author (email: chaogao@zju.edu.cn.)

probes [30], surface-enhanced Raman scattering substrates [31–33], semiconductors [34], and optoelectronic devices [35]. In this respect, graphene oxide (GO) sheets are generally used as the raw materials or precursors of graphene sheets due to their good dispersibility in organic solvents. However, the reported protocols for graphene-metal hybrids are relatively complex which generally require two steps of reduction of GO material and deposition of metal NPs. Besides, there still exists a disputing problem that where the carboxylic acid groups of GO locate. This problem could be possibly resolved by *in situ* deposition of NPs on GO indirectly because the carboxylic acids are normally the nucleation sites for NPs formation. Through such a method, some researchers showed that carboxylic acids were located at the edges of GO since the NPs fringed the GO/reduced graphene sheets [36]. So this could be called "edge view". On the contrary, others revealed that carboxylic acids should be statistically scattered on GO sheets since the NPs were found to be uniformly distributed on the whole sheets (called "whole view") [23, 24, 30]. Recently, our group demonstrated the more validity of the "whole view" by deposition of various NPs [37–39] as well as grafting polymer brushes on GO substrates [40].

In this paper, we report solution-based methods to prepare Pd, Pt, Au, and Ag NPs-decorated graphene nanosheets. The synthesis methods are simple and effective, allowing various kinds of noble metal NPs uniformly anchored on the surfaces of reduced graphene nanosheets. The reduction of GO and the *in situ* deposition of metal NPs were achieved in a one-pot process. Furthermore, the results confirmed the exactness of the "whole view" with the uniform depositions of different metal NPs on GO sheets. The as-prepared nanocatalysts show good disperibility and their catalytic activities were evaluated by the reduction of hexacyanoferrate(III). Our metal-graphene nanohybrids constitute a new class of 2-D hybrid nanocatalysts with promising applications.

2 Experimental

2.1 Materials

Graphite powder (40 μm) was obtained from Qingdao Henglide Graphite Co., Ltd. Graphene oxide (GO) was synthesized from natural graphite powder according to the previous protocol [2, 40, 41]. Ethylene glycol (99%) was purchased from Aldrich and used as received. Palladium(II) chloride ($PdCl_2$, 99%), potassium tetrachloroplatinate (II) (K_2PtCl_4, 99%), gold(III) chloride hydrate ($AuCl_3{\cdot}HCl{\cdot}H_2O$, 99%), silver nitrate ($AgNO_3$, 99%), potassium hexacyanoferrate(III) ($K_3Fe(CN)_6$, 99%), sodium borohydride ($NaBH_4$, 96%), *N*,*N*-dimethyl formamide (DMF), and other solvents were obtained from Sinopharm Chemical Reagent Co., Ltd. (SCRC) and used as received.

2.2 Characterization

Transmission electron microscopy (TEM) analysis was performed on a FEI/Philips CM200 electron microscope operating at 160 kV or a FEI Tecnai G2 F30 S-Twin electron microscope operating at 300 kV. Scanning electron microscopy (SEM) images were obtained on a Hitachi S4800 field-emission SEM system. Atomic force microscopy (AFM) was done using a Digital Instrument Nanoscope IIIa scanning probe microscope, operating at the tapping mode, with samples prepared by spin-coating sample solutions onto freshly cleaved mica substrates at 1500 r/min. The X-ray diffractions (XRD) were recorded on a Philips X'Pert PRO diffractometer equipped with Cu K α radiation (40 kV, 40 mA). Raman spectra were collected on a Jobin-Yvon LabRam HR 800 Raman spectroscope equipped with a 514.5 nm laser source. UV-vis spectra were recorded using a Varian Cary 300 Bio UV-vis spectrophotometer.

2.3 Preparation of graphene-Pd (G-Pd) nanohybrids

GO (10 mg) was dispersed via sonication in 20 mL of ethylene glycol-water solution (3:2 *v*/*v*). $PdCl_2$ (12.8 mg) was added and the mixture was heated at 125 °C under nitrogen for 4 h. The product was separated by centrifugation and washed with ethanol.

2.4 Preparation of graphene-Pt (G-Pt) nanohybrids

GO (10 mg) was dispersed via sonication in 20 mL of ethylene glycol-water solution (3:2 *v*/*v*). K_2PtCl_4 (6.4 mg) was added and the mixture was heated at 125 °C under nitrogen for 4 h. The product was separated by centrifugation and washed with ethanol.

2.5 Preparation of graphene-Au (G-Au) nanohybrids

GO (10 mg) was dispersed via sonication in 30 mL of DMF-water solution (9:1 *v*/*v*). $AuCl_3{\cdot}HCl{\cdot}H_2O$ (6.3 mg) was added and the mixture was stirred for 1 h. The freshly prepared $NaBH_4$ aqueous solution (2 mL, 0.118 M) was slowly added dropwise into the above mixture. The mixture was heated at 80 °C under nitrogen for 4 h. The product was separated by centrifugation and washed with ethanol.

2.6 Preparation of graphene-Ag (G-Ag) nanohybrids

GO (10 mg) was dispersed via sonication in 30 mL of DMF-water solution (9:1 *v*/*v*). $AgNO_3$ (4.8 mg) was added and the mixture was stirred for 1 h. The freshly prepared $NaBH_4$ aqueous solution (2 mL, 0.118 M) was slowly added dropwise into the above mixture. The mixture was heated at 80 °C under nitrogen for 4 h. The product was separated by centrifugation and washed with ethanol.

2.7 Catalysis measurements

In the standard quartz cuvette with a 1 cm path length, double-distilled water (1.0 mL), $K_3Fe(CN)_6$ aqueous solution (8 mM, 0.6 mL), and $NaBH_4$ in 0.1 M NaOH aqueous solution (32 mM, 1.4 mL) were added. The alkaline solution could minimize the decomposition of borohydride [42]. All solutions were previously deaerated and saturated with N_2. After one drop of ethanol solution of graphene-metal nanohybrids (1 mg/mL) was added into the above solution, the absorption spectra were recorded every 30 s in the range of 280–550 nm at room temperature.

3 Results and discussion

3.1 Synthesis of graphene-metal nanoparticles hybrids

The preparation strategy for the graphene-metal nanohybrids is outlined in Scheme 1 (for detailed experimental steps, please see Experimental section). GO was first prepared by oxidization of natural graphite powder. Graphite consists of parallelly stacked flat graphene layers with a plane distance of 0.335 nm. The severe oxidation process destroys the graphite stack and introduces many oxygen-containing groups (e.g., hydroxyl, carboxyl, epoxide, lactone, or ether) onto the GO nanosheets. The as-prepared GO readily exfoliates into individual nanosheets in polar solvents upon sonication, forming stable colloidal suspensions that are stabilized by electrostatic repulsion [43]. The metal ions could be adsorbed on the GO nanosheets by the coordination with the surface functional moieties on GO. Under reduction atmosphere provided by $NaBH_4$ or ethylene glycol at elevated temperature, the metal ions are transformed into crystals and deposited on the surfaces of nanosheets accompanying with the reduction of GO into graphene, affording graphene-metal nanocrystals hybrids. The ethylene glycol reduction system was applied to the synthesis of Pd and Pt nanoparticles on graphene successfully, but it did not work well for the cases of Au and Ag, so the $NaBH_4$ reduction system was used to produce Au and Ag nanoparticles with high crystalline quality and narrow size distribution.

It should be noted that the oxygen functionalities, especially the carboxylic acids, on the GO surface are very important for the preparation of graphene-metal nanohybrids. For one thing, they help to solubilize the nanosheets in solvents and thus the metal ion could readily and evenly coordinate onto nanosheets. For another thing, they provide reactive sites for the nucleation and growth of metal NPs [30]. Moreover, GO has also been reduced to graphene along with the reduction of metal ions in such a one-pot process. Both of the reductive solvents and the metal NPs adsorbed on GO help to reduce GO [24]. The reduction of GO was demonstrated by further characterizations as discussed in the following text and can be also seen from the color of the reaction mixture that changed from yellow-brown to black [44].

3.2 Characterizations of graphene-metal nanoparticles hybrids

The morphology and structure of GO and graphene-metal nanohybrids were characterized by transmission electronic microscopy (TEM). The TEM samples were prepared by dropping just sonicated dispersions in ethanol onto copper grids coated with lacey carbon and dried at room temperature. As seen in Figure 1(a), GO has a typical flake-like shape with slight wrinkles on the surfaces. The TEM images of graphene-metal nanohybrids (Figure 1(b–l)) show the metal nanoparticles appear as dark dots and are uniformly decorated on the graphene sheets in each sample. The distribution of metal nanoparticle on grahpene is quite even, and no big conglomeration of NPs or large undecorated vacancy on graphene was observed in the TEM images. The average diameters of the Pd, Pt, Au, and Ag nanoparticle are 18.8, 2.5, 15.6 and 48.2 nm, respectively. Furthermore, the energy dispersive X-ray spectroscopy (EDS) measurements confirm the presence of corresponding metal elements in each sample as shown in Figure 2. The copper signals in the EDS curves origin from the copper grids that support the samples. It is also found from the EDS measurements that the weight contents of Pd, Pt, Au, and Ag approach 38.6%, 17.5%, 18.2% and 18.3%, respectively. The high contents of metals suggest the high loading efficiency of metals on graphene nanosheets.

Scanning electronic microscopy (SEM) was also used to observe the surface morphology of graphite, GO and graphene-metal nanohybrids. Graphite consists of large stacks as displayed in the SEM image (Figure 3(a)), while GO is exfoliated into thin wrinkled flakes (Figure 3(b)), which is

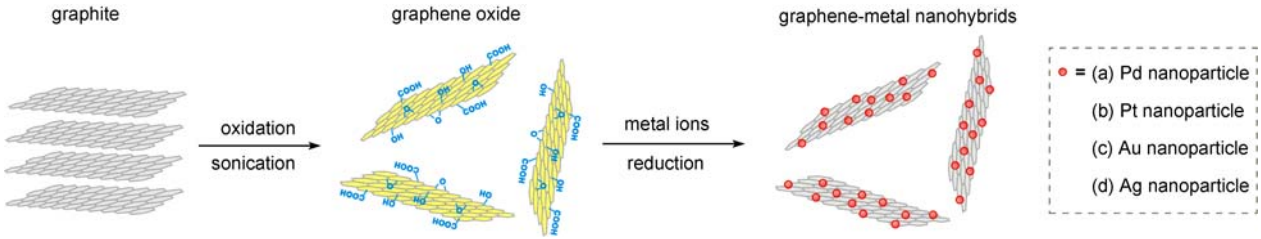

Scheme 1 Schematic description of the preparation of Pd, Pt, Au, and Ag nanoparticles decorated graphene nanosheets.

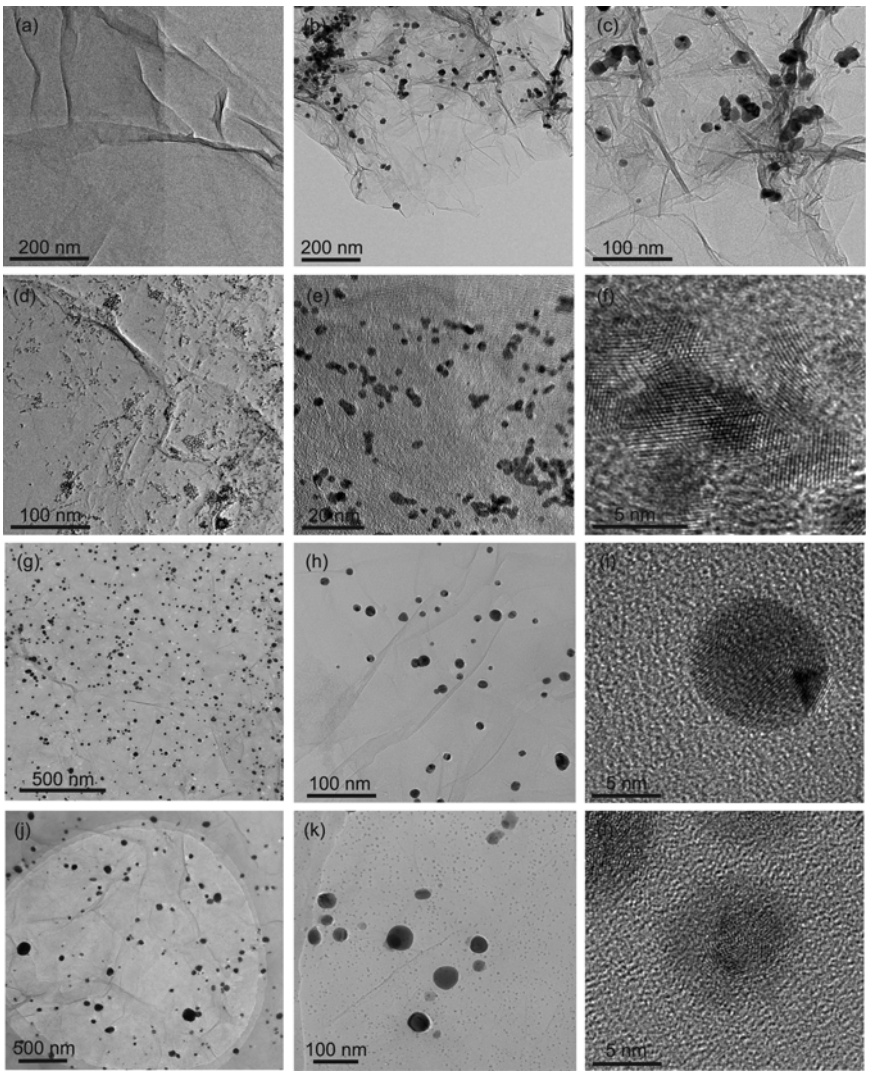

Figure 1 TEM images of GO (a), G–Pd (b, c), G-Pt (d–f), G-Au (g–i) and G-Ag (j–l).

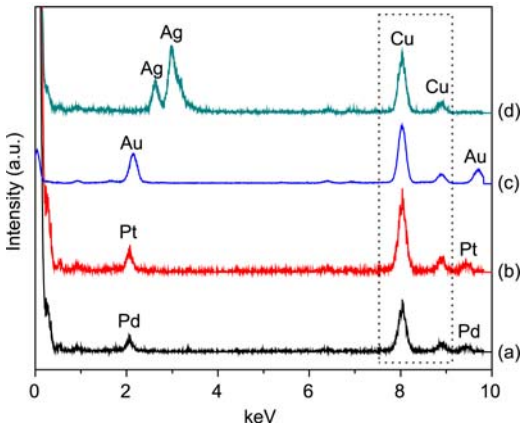

Figure 2 EDS spectra of G-Pd (a), G-Pt (b), G-Au (c) and G-Ag (d).

in accord with its TEM image. Since GO is electrically insulated, it has to be sputtered with Au to form a thin layer of conductive film in order to obtain clear SEM image. In the SEM images of graphene-metal nanohybrids (Figure 3(c)–3(f)), the metal nanoparticles appear as discrete bright dots and homogeneously distribute on the surfaces of graphene. The graphene-metal nanohybrids could be directly characterized by SEM without coated with Au film, suggesting their conductive nature acquired by the reduction of GO to graphene.

The atomic force microscopy (AFM) image in Figure 4(a) displays that the purified GO nanosheets with height of about 0.7–0.8 nm and dimension of several micrometers spread on the mica substrate, demonstrating the single-atom layer structures for our GO materials. The typical AFM images of the Pd, Pt and Au nanoparticles decorated-graphene nanosheets (Figure 4(b)–(d)) show that plenty of round protuberances are distributed on the slightly wrinkled surfaces of graphene, and the nanosheets are mostly isolated single sheets, which are in accord with the TEM and SEM results.

The microscopy observations confirm that the metal NPs are uniformly distributed on the whole graphene sheets,

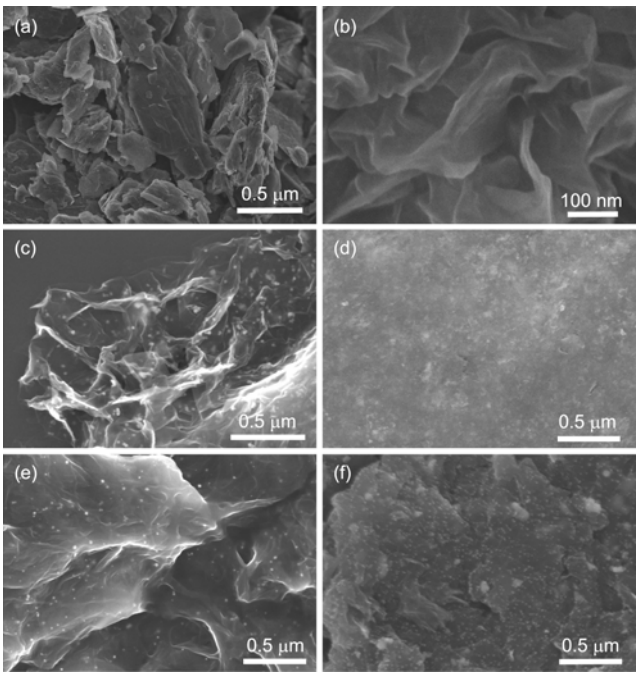

Figure 3 SEM images of graphite (a), GO (b), G-Pd (c), G-Pt (d), G-Au (e) and G-Ag (f).

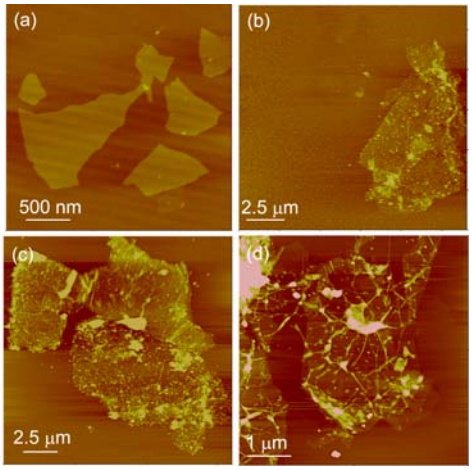

Figure 4 AFM images of GO (a), G-Pd (b), G-Pt (c) and G-Au (d).

indicating in turn that the carboxylic acid groups, the predominant nucleation sites for NPs [37], are statistically or randomly introduced on GO sheets rather than only at the edges during the oxidation of graphite. This conclusion is in good agreement with that obtained by other methods in our group [37–40], which lays the foundation for the preparation of NPs-covered graphene sandwich-like superstructures.

The crystalline structure of metal nanoparticles on graphene was identified by X-ray diffraction (XRD) measurements, and the results are shown in Figure 5. GO shows an obvious diffraction peak at 10.0°, but this peak disappeared and the (002) diffraction peak of graphite reappeared in the

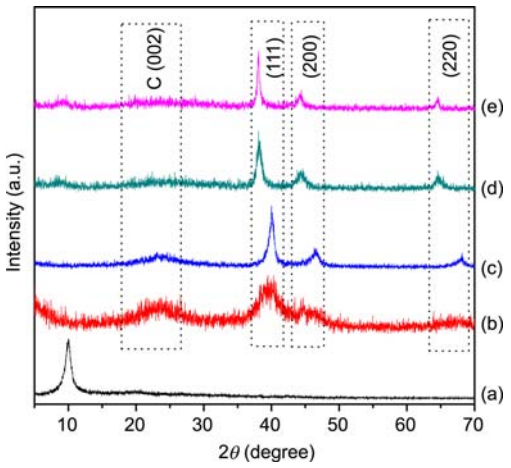

Figure 5 XRD patterns of GO (a), G-Pd (b), G-Pt (c), G-Au (d), and G-Ag (e).

XRD patterns of graphene-metal nanohybrids, which is an indication that GO has been reduced to graphene and restored to an ordered crystalline structure [45]. The metal nanoparticles on the graphene-metal nanohybrids all show characteristic diffraction peaks of (111), (200), and (220) planes in their XRD patterns. The peak positions and relative intensities match well with the standard XRD data for face-centered cubic Pd, Pt, Au, and Ag (JCPDS card 05-0681, 65-2868, 65-2870, 04-0783, respectively).

The significant structural changes of the graphitic substrate during the synthesis process are reflected in the Raman spectra (Figure 6). Raman spectroscopy is commonly used to identify the ordered and disordered crystal structures of carbonaceous materials. Two characteristic bonds are usually observed in a typical Raman spectrum of carbon: the G band around 1580 cm^{-1} corresponds to sp^2-bonded carbon atoms in a hexagonal lattice, and the D band around 1350 cm^{-1} is related to the vibrations of sp^3-carbon atoms of defects and disorder [46]. The Raman spectrum of the natural graphite shows a strong G band and a weak D band with a low D/G intensity ratio of 0.34. In the Raman spectrum of

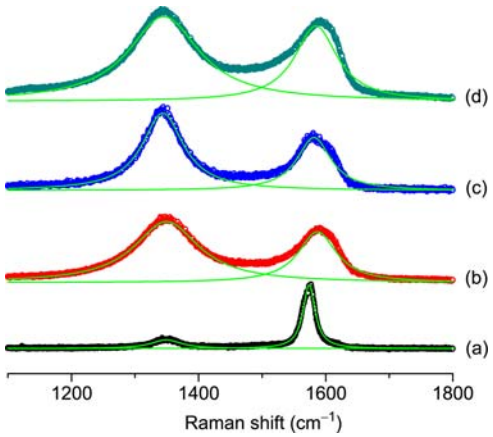

Figure 6 Raman spectra of graphite (a), GO (b), G-Pt (c) and G-Au (d).

GO, the G band is broadened, and the D band becomes bigger with a high D/G intensity ratio of 2.04, revealing the oxidation caused a high level of disorder in the graphene nanosheets. The D/G intensity ratios are 1.78 and 1.88 for G-Pt and G-Au, respectively. The decreased D/G intensity ratios of graphene-metal in comparison with that of GO indicate that new graphitic domains with more numerous in number but smaller in size are generated upon the reduction of GO [47].

The as-prepared graphene-metal nanohybrids have good dispersibility in solvents such as ethanol, water, and *N*,*N*-dimethylformamide (DMF) (Figure 7). Notably, the pure graphene sheets prepared in the control experiments without adding of metal ions are insoluble in solvents. This is due to the pure reduced graphene sheets tend to aggregate in solvent due to the strong van der Waals interactions, while the metal nanoparticles on the graphene sheets act as spacers that could prevent the aggregation while drying. This effect of metal nanoparticles on graphene has also been indicated in the previous reports [23, 34]. The improved disperibility of graphene-metal nanohybrids with respect to graphene greatly enlarges their applications in many fields, including solution processing, solution catalysis, and so forth.

3.3 Catalysis investigations of graphene-metal nanoparticles hybrids

In order to test the catalysis activity of the graphene-metal nanohybrids, we employed a model electron-transfer reaction of reducing hexacyanoferrate(III) by borohydride ions in aqueous solution [42]. The redox reaction is depicted as chemical eq. (1) [48]:

$$BH_4^- + 8\left[Fe(CN)_6\right]^{3-} + 3H_2O \rightarrow H_2BO_3^- + 8\left[Fe(CN)_6\right]^{4-} + 8H^+ \quad (1)$$

In the presence of noble metal nanoparticles, the catalysis mechanism involves a two-step process as shown in eqs. (2) and (3) [49]:

$$BH_4^- + \text{Metal} \leftrightarrow Q^- (\text{fast}) \quad (2)$$

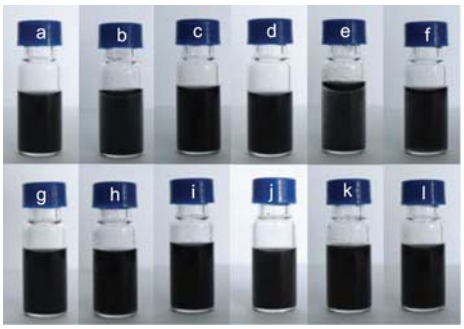

Figure 7 Photographs of G-Pd (a–c), G-Pt (d–f), G-Au (g–i), and G-Ag (j–l) in ethanol (a, d, g, j), water (b, e, h, k) and DMF (c, f, i, l).

$$Q^- + \left[Fe(CN)_6\right]^{3-} \rightarrow \left[Fe(CN)_6\right]^{4-} + Q \ (\text{slow}) \quad (3)$$

The metal NPs firstly undergo cathodic polarization by borohydride rapidly, and in the next slow step, their excess surface electrons transfer to the ferricyanide ions that diffuse toward the metal nanoparticles. It should be noted that the noncatalyzed reaction of eq. (1) can be neglected since it is much slower than the catalyzed reaction of eqs. (2) and (3).

In the experimental runs, the concentration of $NaBH_4$ was set to in large excess as compared to hexacyanoferrate(III) ions. Thus, the kinetics of the reduction process can be regarded as a pseudo-first-order reaction. The progression of the reaction was monitored indirectly through the ultraviolet-visible UV-vis spectrum of hexacyanoferrate (III). The characteristic absorption peak of hexacyanoferrate(III) is located at 420 nm, and its intensity was continuously decreased immediately after the addition of graphene-metal nanohybrids, revealing the occurrence of catalyzed reduction. As seen in Figure 8, the UV-vis spectra were recorded per 0.5 min for each sample of G-Pd, G-Pt, G-Au, and G-Ag, and all of the absorption peaks of hexacyanoferrate(III) decreased quickly and completely disappeared within about 5 min. The insets of Figure 8 demonstrate that the experimental data fit well with the integrated first-order kinetics of eq. (4):

$$In\left(\frac{A_t - A_\infty}{A_0 - A_\infty}\right) = -k_{obs}t \quad (4)$$

where t is the reaction time, A_0 is the initial absorbance at time zero, A_t is the absorbance at time t, A_∞ is the absorbance when the reaction is completed, and k_{obs} is the observed rate constant. The k_{obs}s of these reactions for G-Pd, G-Pt, G-Au and G-Ag are calculated to be 9.5×10^{-3}, 2.1×10^{-2}, 1.2×10^{-2}, and 2.6×10^{-2} s^{-1}, respectively. The data are comparable to the previously reported values for Pt NPs supported on CNTs (~10^{-2}–10^{-1} s^{-1}) [50] and Au NPs supported on SiO_2 or TiO_2 hollow capsules (~10^{-3}–10^{-2} s^{-1}) [49] for the same chemical reaction. It can be seen that the noble metal NPs still possess high catalytic activities after being anchored on graphene. The graphene nanosheets could prevent the metal nanoparticles from aggregation, and also sever as large, flat, and highly stable substrates, enabling the reactions proceed favourably on the exteriors of metal NPs. In addition, the graphene-metal nanohybrids could be easily separated from the reaction system by filtration or centrifugation and reused, which shows the advantages of using the graphene nanosheets as the catalyst support.

4 Conclusions

In summary, we showed that graphene-metal (Pd, Pt, Au and Ag) nanohybrids can be facilely synthesized in solution

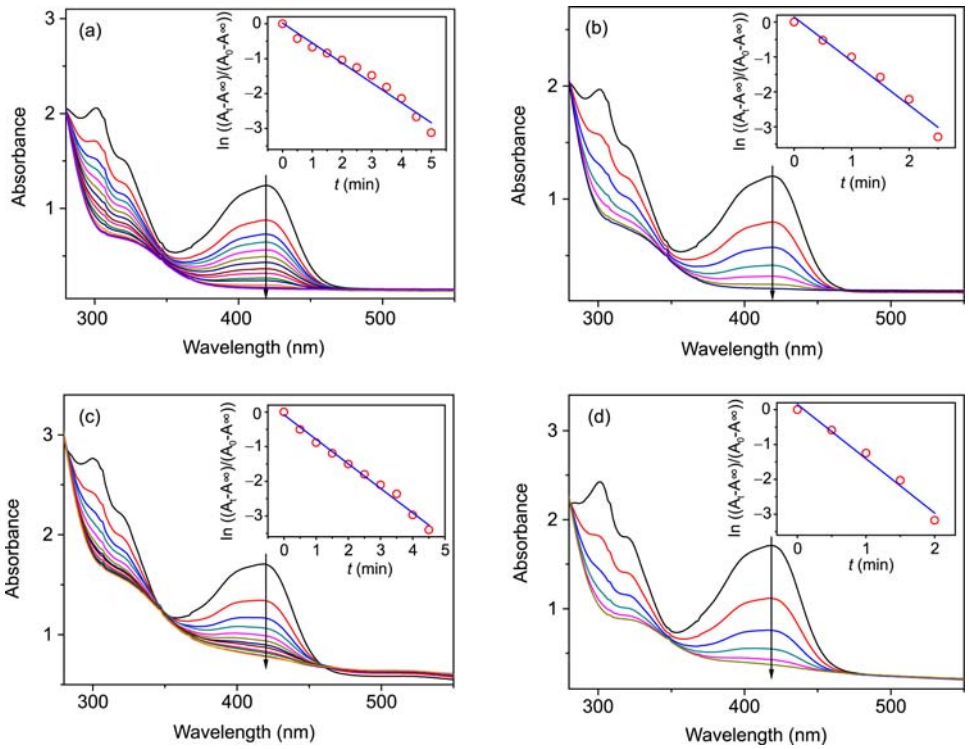

Figure 8 Successive UV-vis spectra of the mixture of hexacyanoferrate(III) and sodium borohydride upon addition of graphene-metal nanohybrids: (a) G-Pd, (b) G-Pt, (c) G-Au and (d) G-Ag. The insets show the good fit of the experimental results to first-order analysis according to eq. (4).

with GO as the precursor. In the synthesis process, the reduction of GO and the formation of metal NPs are accomplished simultaneously. The metal NPs that are uniformly anchored on the surfaces of individual graphene nanosheets could prevent the restacking of graphene, resulting in good dispersibility in solvents. All of the as-prepared graphene-metal samples show catalysis activity in the catalytic reduction of potassium hexacyanoferrate(III). This study could be extended to other graphene-metal nanohybrids with promising applications such as direct methanol fuel cells. Further research in this direction is currently underway.

This work was financially supported by the National Natural Science Foundation of China (50773038& 20974093), National Basic Research Program of China (973 Program, 2007CB936000), Qianjiang Talent Foundation of Zhejiang Province (2010R10021), the Fundamental Research Funds for the Central Universities (2009QNA4040), and the Foundation for the Author of National Excellent Doctoral Dissertation of China (200527).

1 Geim AK, Novoselov KS. The rise of graphene. *Nat Mater*, 2007, 6: 183–191
2 Park S, Ruoff RS. Chemical methods for the production of graphenes. *Nature Nanotechnol*, 2009, 4: 217–224
3 Rao CNR, Sood AK, Subrahmanyam KS, Govindaraj A. Graphene: The new two-dimensional nanomaterial. *Angew Chem Int Ed*, 2009, 48: 7752–7777
4 Dreyer DR, Park S, Bielawski CW, Ruoff RS. The chemistry of graphene oxide. *Chem Soc Rev*, 2010, 39: 228–240
5 Allen MJ, Tung VC, Kaner RB. Honeycomb carbon: A review of graphene. *Chem Rev*, 2010, 110: 132–145
6 Katsnelson MI. Graphene: Carbon in two dimensions. *Mater Today*, 2007, 10: 20–27
7 Cravotto G, Cintas P. Sonication-assisted fabrication and post-synthetic modifications of graphene-like materials. *Chem Eur J*, 2010, 16: 5246–5259
8 Soldano C, Mahmood A, Dujardin E. Production, properties and potential of graphene. *Carbon*, 2010, 48: 2127–2150
9 Stoller MD, Park SJ, Zhu YW, An JH, Ruoff RS. Graphene-based ultracapacitors. *Nano Lett*, 2008, 8: 3498–3502
10 Lu GH, Mao S, Park S, Ruoff RS, Chen JH. Facile, Noncovalent decoration of graphene oxide sheets with nanocrystals. *Nano Res*, 2009, 2: 192–200
11 Liu JB, Fu SH, Yuan B, Li YL, Deng ZX. Toward a universal "adhesive nanosheet" for the assembly of multiple nanoparticles based on a protein-induced reduction/decoration of graphene oxide. *J Am Chem Soc*, 2010, 132: 7279–7281
12 Burda C, Chen XB, Narayanan R, El-Sayed MA. Chemistry and properties of nanocrystals of different shapes. *Chem Rev*, 2005, 105: 1025–1102
13 Astruc D, Lu F, Aranzaes JR. Nanoparticles as recyclable catalysts: The frontier between homogeneous and heterogeneous catalysis. *Angew Chem Int Ed*, 2005, 44: 7852–7872
14 Stakheev AY, Kustov LM. Effects of the support on the morphology and electronic properties of supported metal clusters: Modern concepts and progress in 1990s. *Appl Catal A*, 1999, 188: 3–35
15 Felpin FX, Ayad T, Mitra S. Pd/C: An old catalyst for new applications – Its use for the Suzuki-Miyaura reaction. *Eur J Org Chem*, 2006: 2679–2690
16 Serp P, Corrias M, Kalck P. Carbon nanotubes and nanofibers in catalysis. *Appl Catal A*, 2003, 253: 337–358
17 Liang CH, Xia W, van den Berg M, Wang YM, Soltani-Ahmadi H, Schluter O, Fischer, RA, Muhler M. Synthesis and catalytic performance of Pd nanoparticle/functionalized CNF composites by a

two-step chemical vapor deposition of Pd(allyl)(Cp) precursor. *Chem Mater*, 2009, 21: 2360–2366
18 Karousis N, Tsotsou GE, Evangelista F, Rudolf P, Ragoussis N, Tagmatarchis N. Carbon nanotubes decorated with palladium nanoparticles: Synthesis, characterization, and catalytic activity. *J Phys Chem C*, 2008, 112: 13463–13469
19 Gao C, He H, Zhou L, Zheng X, Zhang Y. Scalable functional group engineering of carbon nanotubes by improved one-step nitrene chemistry. *Chem Mater*, 2009, 21: 360–370
20 Novoselov KS, Geim AK, Morozov SV, Jiang D, Zhang Y, Dubonos SV, Grigorieva IV, Firsov AA. Electric field effect in atomically thin carbon films. *Science*, 2004, 306: 666–669
21 Scheuermann GM, Rumi L, Steurer P, Bannwarth W, Mulhaupt R. Palladium nanoparticles on graphite oxide and its functionalized graphene derivatives as highly active catalysts for the Suzuki-Miyaura coupling reaction. *J Am Chem Soc*, 2009, 131: 8262–8270
22 Li Y, Fan X, Qi J, Ji J, Wang S, Zhang G, Zhang F. Palladium nanoparticle–graphene hybrids as active catalysts for the Suzuki reaction. *Nano Res*, 2010, 3: 429–437
23 Si YC, Samulski ET. Exfoliated graphene separated by platinum nanoparticles. *Chem Mater*, 2008, 20: 6792–6797
24 Xu C, Wang X, Zhu JW. Graphene-metal particle nanocomposites. *J Phys Chem C*, 2008, 112: 19841–19845
25 Li YJ, Gao W, Ci LJ, Wang CM, Ajayan PM. Catalytic performance of Pt nanoparticles on reduced graphene oxide for methanol electro-oxidation. *Carbon*, 2010, 48: 1124–1130
26 Dong LF, Gari RRS, Li Z, Craig MM, Hou SF. Graphene-supported platinum and platinum-ruthenium nanoparticles with high electrocatalytic activity for methanol and ethanol oxidation. *Carbon*, 2010, 48: 781–787
27 Guo SJ, Dong SJ, Wang EW. Three-dimensional Pt-on-Pd bimetallic nanodendrites supported on graphene nanosheet: Facile synthesis and used as an advanced nanoelectrocatalyst for methanol oxidation. *ACS Nano*, 2010, 4: 547–555
28 Kong BS, Geng JX, Jung HT. Layer-by-layer assembly of graphene and gold nanoparticles by vacuum filtration and spontaneous reduction of gold ions. *Chem Commun*, 2009: 2174–2176
29 Hong WJ, Bai H, Xu YX, Yao ZY, Gu ZZ, Shi GQ. Preparation of gold nanoparticle/graphene composites with controlled weight contents and their application in biosensors. *J Phys Chem C*, 2010, 114: 1822–1826
30 Goncalves G, Marques P, Granadeiro CM, Nogueira HIS, Singh MK, Gracio J. Surface modification of graphene nanosheets with gold nanoparticles: The role of oxygen moieties at graphene surface on gold nucleation and growth. *Chem Mater*, 2009, 21: 4796–4802
31 Shen JF, Shi M, Li N, Yan B, Ma HW, Hu YZ, Ye MX. Facile synthesis and application of Ag-chemically converted graphene nanocomposite. *Nano Res*, 2010, 3: 339–349
32 Xu C, Wang X. Fabrication of flexible metal-nanoparticte film using graphene oxide sheets as substrates. *Small,* 2009, 5: 2212–2217
33 Zhou XZ, Huang X, Qi XY, Wu SX, Xue C, Boey FYC, Yan QY, Chen P, Zhang H. *In situ* synthesis of metal nanoparticles on single-layer graphene oxide and reduced graphene oxide surfaces. *J Phys Chem C*, 2009, 113: 10842–10846
34 Pasricha R, Gupta S, Srivastava AK. A facile and novel synthesis of Ag-graphene-based nanocomposites. *Small,* 2009, 5: 2253–2259
35 Muszynski R, Seger B, Kamat PV. Decorating graphene sheets with gold nanoparticles. *J Phys Chem C*, 2008, 112: 5263–5266
36 Yuge R, Zhang MF, Tomonari M, Yoshitake T, Iijima S, Yudasaka M. Site identification of carboxyl groups on graphene edges with Pt derivatives. *ACS Nano*, 2008, 2: 1865–1870
37 He HK, Gao C. General approach to individually dispersed, highly soluble, and conductive graphene nanosheets functionalized by nitrene chemistry. *Chem Mater*, 2010, 22: 5054–4064
38 He HK, Gao C. Supraparamagnetic, conductive and processable multifunctional graphene nanosheets coated with high-density Fe_3O_4 nanoparticles. *ACS Appl Mater Interf*, 2010, 2: 3201–3210
39 Kou L, Gao C. Making silica nanoparticles-covered graphene oxide nanohybrids as general building blocks for large-area superhydrophilic coatings. *Nanoscale*, in press, c0nr00609b
40 Xu Z, Gao C. *In situ* polymerization approach to graphene-reinforced nylon-6 composites. *Macromolecules*, 2010, 43: 6716–6723
41 Hummers WS, Offeman RE. Preparation of graphitic oxide. *J Am Chem Soc*, 1958, 80: 1339–1339
42 Carregal-Romero S, Buurma NJ, Perez-Juste J, Liz-Marzan LM, Herves P. Catalysis by Au@PNIPAM nanocomposites: Effect of the cross-linking density. *Chem Mater*, 2010, 22: 3051–3059
43 Li D, Muller MB, Gilje S, Kaner RB, Wallace GG. Processable aqueous dispersions of graphene nanosheets. *Nature Nanotechnol,* 2008, 3: 101–105
44 Williams G, Seger B, Kamat PV. TiO_2-graphene nanocomposites. UV-assisted photocatalytic reduction of graphene oxide. *ACS Nano*, 2008, 2: 1487–1491
45 Wang GX, Yang J, Park J, Gou XL, Wang B, Liu H, Yao J. Facile synthesis and characterization of graphene nanosheets. *J Phys Chem C*, 2008, 112: 8192–8195
46 Shen JF, Hu YZ, Shi M, Li N, Ma HW, Ye MX. One step synthesis of graphene oxide-magnetic nanoparticle composite. *J Phys Chem C*, 2010, 114: 1498–1503
47 Li FH, Song JF, Yang HF, Gan SY, Zhang QX, Han DX, Ivaska A, Niu L. One-step synthesis of graphene/SnO_2 nanocomposites and its application in electrochemical supercapacitors. *Nanotechnology*, 2009, 20: 455602
48 Carregal-Romero S, Perez-Juste J, Herves P, Liz-Marzan LM, Mulvaney P. Colloidal gold-catalyzed reduction of ferrocyanate (III) by borohydride ions: A model system for redox catalysis. *Langmuir*, 2010, 26: 1271–1277
49 Pastoriza-Santos I, Perez-Juste J, Carregal-Romero S, Herves P, Liz-Marzan LM. Metallodielectric hollow shells: Optical and catalytic properties. *Chem Asian J*, 2006, 1: 730–736
50 Sanles-Sobrido M, Correa-Duarte MA, Carregal-Romero S, Rodriguez-Gonzalez B, Alvarez-Puebla RA, Herves P, Liz-Marzan LM. Highly catalytic single-crystal dendritic Pt nanostructures supported on carbon nanotubes. *Chem Mater*, 2009, 21: 1531–1535